Title
LARGE-AREA HIGH-CURRENT ION SOURCE

Authors
Baker, W.R.
Ehlers, K.W.
Kunkel, W.B.
et al.

Publication Date
1971-08-01

To be presented at the Symposium
on Ion Sources and Formation of
Ion Beams, BNL, Upton, NY,
October 19-21, 1971

LBL-35 c. 2
Preprint

LARGE-AREA HIGH-CURRENT ION SOURCE

W. R. Baker, K. W. Ehlers, W. B. Kunkel, and A. F. Lietzke

August 1971

AEC Contract No. W-7405-eng-48

LAWRENCE RADIATION LABORATORY
UNIVERSITY of CALIFORNIA BERKELEY

LARGE-AREA HIGH-CURRENT ION SOURCE*

W. R. Baker, K. W. Ehlers, W. B. Kunkel, and A. F. Lietzke

Lawrence Berkeley Laboratory
Berkeley, California 94720

Abstract

Neutral injection, a method of producing and heating plasmas in certain controlled-fusion experiments, requires the development of multi-ampere ion sources. We are reporting the development of a new type of ion source geometry capable of delivering a high ion current density over a large extraction area. Probes used to determine the operating characteristics of the model tested indicate the availability of noise-free ion current densities in excess of 1 A/cm^2 and flat to ± 15% over a 4-cm diameter. A larger version of the model tested is being designed to deliver a 30-msec 20-A, 20-keV deuterium ion beam for the Livermore 2X-II experiment.

Introduction

The injection of large currents of energetic neutral deuterium beams into several controlled-fusion experiments requires the development of high-current ion sources compatible with accelerating structures capable of producing such beams.

Our effort has been directed toward the development of a usable deuterium ion beam current of 20 A with an energy of 20 keV for injection into the 2XII experiment.[1] Operation with 2X II requires beam pulses of from .03 to .1 sec, which allows the use of pulse lines for arc and extractor supplies and reduces the source cooling requirements. Gas pulsing is also necessary since the gas required for the beam current alone is very large. (Allowing an average of one charge per molecule for the three charge states expected–D^+, D_2^+, D_3^+–and no allowance for probable source inefficiencies, a 20-A beam represents a gas flow rate of nearly 300 cm^3/min (STP) or 3600 µl/sec.)

Even though extraction current densities as large as 1 A/cm^2 are contemplated, beam currents of this magnitude require a very large extraction area. The extraction ion optics are very sensitive to the plasma density, and in order to have the extracted beam be usable, the source must be capable of generating the required density sufficiently uniform over the entire extraction region.[2]

Tentatively, the limits of plasma-density variation over this region have been set at ± 15%. In addition, plasma-density variations with time should not exceed this figure. Therefore fluctuations or noise of the type and frequency encountered with most source geometries should be avoided.

Sources capable of producing beam currents of the desired magnitude have not been reported, and thus an indication as to the best type of source geometry to employ was not available. The first type of source constructed was one basically similar to the MATS concept,[3] except that the magnetic field from the anode to the extraction apertures was carefully tailored to allow the plasma to expand to approximately four times the extraction area. The ion current density in the extraction region was found to be sufficiently uniform, but adequate current density could not be achieved over this expanded area. Two other changes involved the use of a large thermally emitting, oxide-coated cathode and a minimum of magnetic field. These changes were expected to reduce arc fluctuations believed to be caused by "cathode spotting" (large currents from small areas) and mutually perpendicular electric and magnetic fields. The quiet reproducible operation obtained with these changes support this reasoning.

Modifications of this original source design, as well as the use of probes to monitor source operation, were instrumental in revealing that substantial ion density was available, even without a magnetic field. This experience led to the design and construction of a source having simplified geometry, which we believe will be capable of fulfilling the difficult requirements. It is basically an electron-bombardment-type ion source operating with a distributed thermionic cathode and somewhat resembles the plasma source of Taylor, Ikezi, and Mac Kenzie.[4]

A photograph of the source reported is shown in Fig. 1, and a block diagram of the source and its associated electronics is shown in Fig. 2.

Design

The oxide-coated cathode has been abandoned in favor of tungsten filaments, because of inadequate emission. In our model there are 8 hairpin filaments (diameter = .11 cm, length = 11 cm) placed in a 5.7-cm-diameter circle inside a conducting cylindrical chamber (diameter = 7 cm, depth = 5.7 cm). At approximately 3000°K these filaments are capable of supplying in excess of 500 A (17 A/cm^2) and require 5 kW of heater power. Power is delivered by a pulsed 3 phase ∇, ∇-connected step-down transformer that is bridge rectified and partially filtered by a 120,000-µF capacitor pack. At the temperature equilibration time of 4 sec, the heater power to each

---

*Work done under the auspices of the U. S. Atomic Energy Commission.

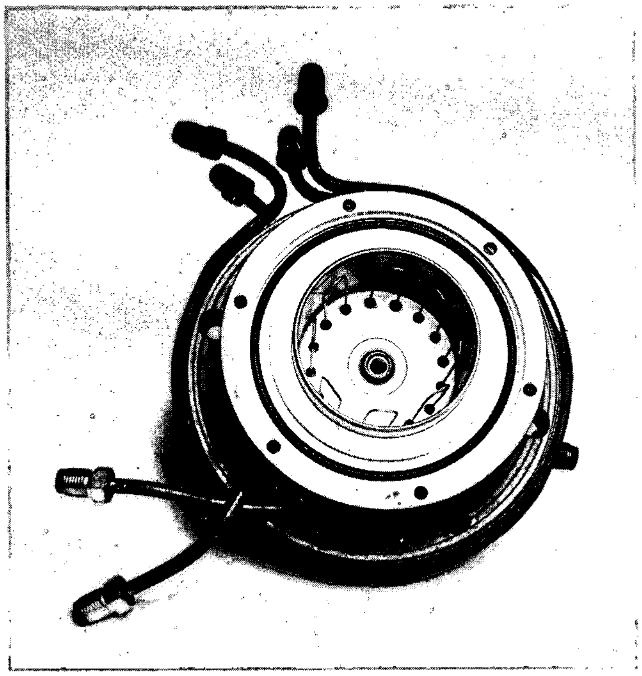

Fig. 1. Source geometry, end view.

filament is 71 A at 8.8 V. Direct-current filament power was used to avoid ac modulation of source potentials.

Two relevant filament design considerations should be noted. First, the large radiant heat load from tungsten filaments not only aggravates general cooling requirements, but can be expected to warp delicate and accurately machined extractor structures. Minimization of this heat load can be done by using the knowledge that electron emission increases more rapidly with temperature than with radiant emission. The reduction of filament area concurrently with increasing temperature is constrained by a second consideration: Tungsten sublimation becomes a problem at high temperatures because of increased impurities as well as the gradual change in filament characteristics.

The anode is located on the axis at one end of the cylinder, opposite the side from which ions are to be extracted. It consists of a copper cylinder (o.d. = .95 cm, i.d. = .6 cm) of sufficient length to allow cooling and vacuum sealing. It subtends an electron collecting area of .79 cm^2, surrounded by a 1.0-cm-i.d. quartz tube.

Several considerations enter into the anode design. Electron-bombardment ionizers are

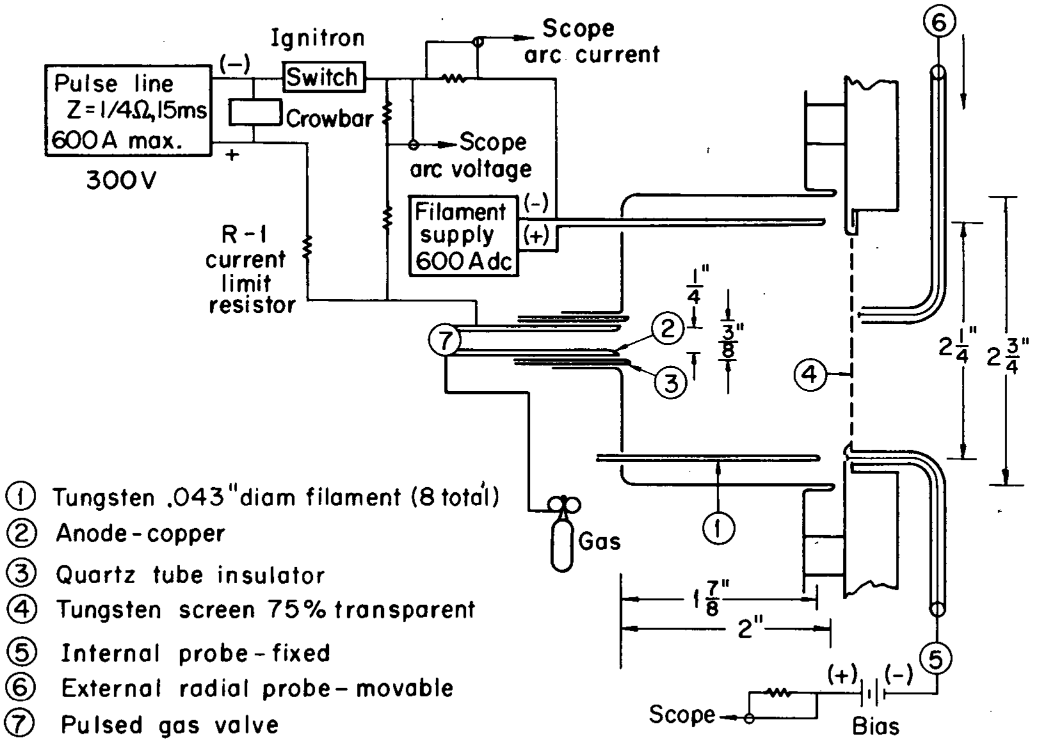

Fig. 2. Block diagram.

efficient to the extent that the primary (energetic) electrons path length—before losing energy to excitation, dissociation, or surfaces—approaches or exceeds the mean free path for ionization. A more precise statement, for a simple case, is made in the Appendix, where it is shown that optimum electron efficiency is obtained by maximizing $n_0 \lambda_u$, where n_0 = neutral density, λ_u=mean useful path length, and optimum gas efficiency occurs by maximizing $I_e' \lambda_u$, where I_e' = primary electron current. λ_u is maximized by minimizing the anode area or by maximizing the electron path length between reflections within the ionization volume. However, anode power dissipation limits cannot be exceeded without anode damage and plasma contamination. Hence for any given current level, a minimum area exists. If the anode current is forced to exceed its incident random electron current, an anode sheath will develop, thereby increasing the power dissipation of the anode and possibly leading to anode damage as well as instabilities. The incident random electron current can be increased by the introduction of higher-pressure gas at the anode. The "hollow anode" design has kept the anode fall at a minimum by introducing the gas at this point.

Gas flow was controlled by a solenoid valve in series with a needle valve connected to a regulated 25-psi deuterium reservoir.

Arc power is supplied from a pulse line composed of iron-core inductors and electrolytic condensers ($Z = 1/4\Omega$). The pulse line is crowbarred after 15 msec to remove the possibility of capacitor damage which would result from voltage reversal. Arc current is controlled by current-limiting resistors as well as the pulse-line voltage-charging level. Typical are waveforms are shown in Fig. 3.

The pulse timing sequence is as follows: Filament on at -4 sec, gas pulsed on at t = -20 msec, arc power on at t = 0, arc power off at t = +15 msec, gas and filament off at t = +30 msec. With the exception of some starting difficulty, pulse-line droop, and filament ripple (Fig. 3), arc operation has been smooth, noise free, and reproducible, with gas flow, arc current, and filament temperature as control parameters.

Results and Discussion

A parallel experimental and theoretical effort to determine an optimum ion extraction geometry has been underway.[2] The results of this work should allow the design of an accel-decel extraction system consisting of arrays of multiple holes or slots, which when combined with the proper gradients and plasma density should provide an ion beam of minimum divergence. Since this system as well as the pulsed high-voltage high-current power supply have not been available, source operation has been determined by means of probes. Two button probes are shown in Fig. 2. One probe is fixed at the radius of the filament circle and the other is radially movable outside of the screened extraction plane. This probe, normally positioned at r = 0, is used to scan the plasma density profile, out to the limit of the 2-in.-diameter screened aperture.

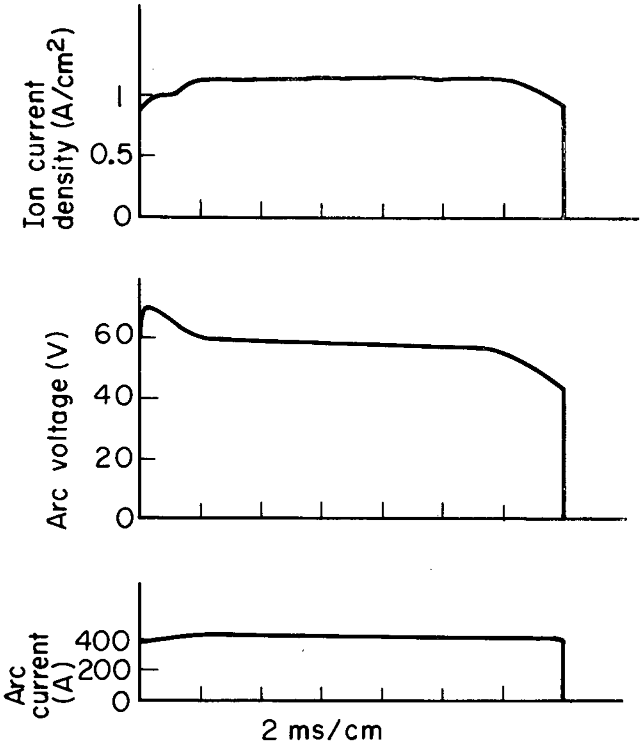

Fig. 3. Typical waveforms.

Figure 4 is a plot of ion current density as read by the radial probe at r = 0. As can be seen, the ion current density increase with arc current is somewhat greater than linear, with the desired current density of $1\ \mathrm{A/cm^2}$ being generated with an arc current of about 300 A.

Figure 5 is a plot of a typical plasma density profile with the arc operating at 470 A.

This profile is within ± 14% of its average out to a 2-cm radius. An integration of the useful ion current in Fig. 5 indicates that 20 A of beam current is available in this 12-cm^2 area. A beam extracted from this area would, however, be reduced by recombination on the extractor structure whose transparency in our present designs will vary from 40% for multiple-hole arrays to 67% for multiple parallel slots. This indicates that the source tested should be capable of producing an accelerated ion beam current of about 10 A.

Shot-to-shot reproducibility has proven to be excellent. Scope traces of numerous successive shots are routinely photographed while taking profile data, and these appear coincident, even in fine detail. In addition to being reproducible, the probe signals are essentially flat in time and noise free.

With large ion-extraction areas, good gas efficiency is required, since there is a minimum of structure separating the gas pressure required

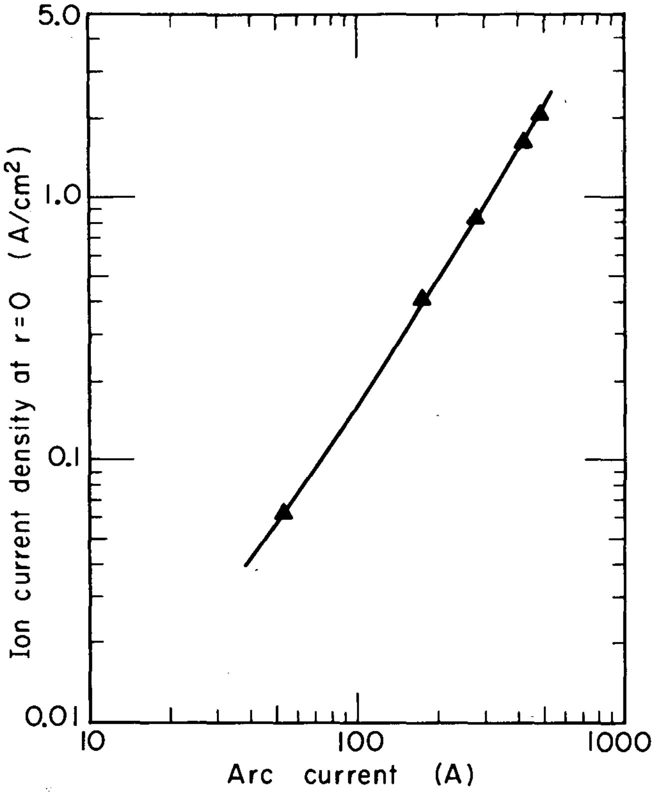

Fig. 4. Ion current density vs arc current.

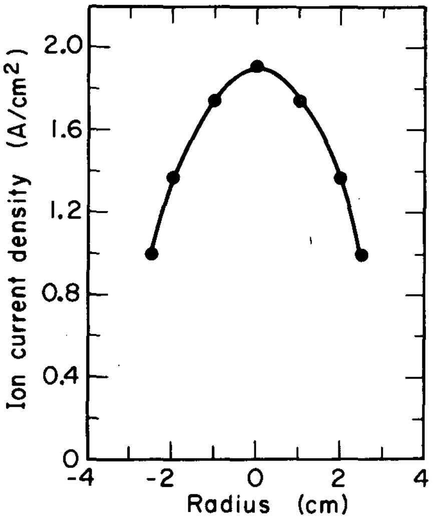

Fig. 5. Ion current density profile.

by the source from the high voltage on the extractor electrodes. Reliable pulsed gas-pressure measurements are difficult to obtain; however, gas flow measurements compared with the integrated probe ion current readings indicate a source-gas efficiency of about 30%. The source pressure requirements seem to be well within the pressure region tested for voltage-holding capability by the group working on extractor design.[2]

Construction is now under way on a larger source utilizing 20 hairpin filaments on a 5-in.-diameter circle. These filaments, all in parallel, will require about 1500 A of heater current. A pulse-line for the arc capable of delivering 1000 A for 30 msec has been constructed and tested. The extractor electrode design utilizing slots has been completed and tests to determine the effects of heat and voltage on similar structures are underway. A pulsed extractor supply capable of supplying 20 A at 20 kV is nearing completion.

Appendix

A precise statement about the importance of the primary electron's mean useful path length can be made in the following simple case. Consider a volume, defined by a simple closed surface, that contains a partially ionized, single-species gas. An electron source injects into the plasma, monoenergetic electrons with an energy sufficient for one ionization or one excitation; the electrons are then contained by reflecting walls or collected by the anode. If p_1 denotes the average probability for anode collection between reflections, one can assign an approximate probability for anode collection survival after N reflections as $P_N \approx e^{-p_1 N}$, a good approximation for $p_1 << 1$. Likewise, if σ_i and σ_x denote the electron-bombardment ionization and excitation cross sections, the probabilities for surviving each effect for a distance s in a uniform gas are

$$P_i = e^{-n_0 \sigma_i s}$$

and

$$P_x = e^{-n_0 \sigma_x s} .$$

Hence, the probability for primary-electron survival of all three independent annihilations within a distance s is

$$P_p = P_a P_i P_x = e^{-[n_0(\sigma_i + \sigma_x) + p_1 N(s)]} .$$

Assigning $N(s) = s/\bar{d}$ ($\bar{d}$ = average path length between reflections), one can define a mean useful path length λ_u

$$\lambda_u = \frac{1}{\frac{p_1}{\bar{d}} + n_0(\sigma_i + \sigma_x)} .$$

This parameter is also significant in the more general case of multiple ionizations per electron where, with the assumptions of constant σ_i, σ_x over the energy range of significance, one can obtain a probability for primary electron survival by a path length s of

$$P_p(s) = e^{-s/\lambda_u}\left[1 + \frac{s}{\lambda_{ie}} + \frac{1}{2}\,\frac{s^2}{\lambda_{ie}^2} + \cdots\right],$$

where $\lambda_{ie} = \dfrac{1}{n_0(\sigma_i + \sigma_x)}$.

The effect that this parameter has upon source efficiency can be illustrated by the following estimation: the steady-state ion continuity equation requires that

$$\operatorname{div} \vec{J}_i = e\, n_0 n_e' \langle \sigma_i v_e \rangle',$$

where $\vec{J}_i$ = ion current density,
n_0 = neutral density,
n_e' = primary electron density,
$\langle \sigma_i v_e \rangle'$ = appropriate average of the ionization cross section over the primary electron velocity distribution.

The primary electron density can be estimated as

$$n_e' \approx \frac{I_e'}{eV}\,\tau',$$

where I_e' = primary electron current,
V = source volume,
$\tau' = \dfrac{\lambda_u}{\langle v_e \rangle'}$ = average primary lifetime.

Integration of the continuity equation over the volume, assuming uniform densities, gives the ion current to the confining surface:

$$\oint \vec{J}_i \cdot d\vec{A} = n_0 I_e' \lambda_u \frac{\langle \sigma_i v_e \rangle'}{\langle v_e \rangle'}.$$

For any given electron velocity distribution, electron efficiency is therefore optimized by maximizing

$$n_0 \lambda_u = \frac{1}{\dfrac{p_1}{n_0 \bar{d}} + \sigma_i + \sigma_x}.$$

Likewise, gas efficiency is optimized by maximizing

$$I_e' \lambda_u = \frac{I_e'}{\dfrac{p_1}{\bar{d}} + n_0(\sigma_i + \sigma_x)}.$$

In the case of negligible magnetic fields, p_1 may be assigned the likely value

$$p_1 = \frac{\text{anode area}}{\text{total surface area}}$$

and $\bar{d}$ the likely value of the typical distance between reflections inside the ionization chamber. Conversely, in a reflex arc, one has $p_1 \approx 1$, while $\bar{d}$ is vastly increased by the application of a strong axial magnetic field.

References

1. F. H. Coensgen et al., Plasma Containment in the LRL 2X-II Experiment, IAEA/CN-28/G12, Madison, Wisconsin, June 1971.
2. W. S. Cooper, K. N. Berkner, and R. V. Pyle, Multiple-Aperture Extractor Design for Producing Intense Ion and Neutral Beams. Lawrence Radiation Laboratory Report UCRL-20698, June 1971.
3. J. E. Osher and G. W. Hamilton, Bull. Am. Phys. Soc. 15, 1441 (1970).
4. R. J. Taylor, H. Ikezi, and K. R. MacKenzie, in Proceedings International Conference on Physics of Quiescont Plasmas, Paris, Sept. 1969.

TECHNICAL INFORMATION DIVISION
LAWRENCE BERKELEY LABORATORY
UNIVERSITY OF CALIFORNIA
BERKELEY, CALIFORNIA 94720